Materials Science, Vol. 20, No. 1, 2002

Highly porous aerogels of very low permeability*

J. PHALIPPOU**, T. WOIGNIER, R. SEMPÉRÉ, P. DIEUDONNÉ

Laboratoire des Verres – UMR CNRS 5587, Université de Montpellier 2,
Place Eugène Bataillon, 34095 Montpellier Cedex 5, France

In this paper, we firstly investigate the way the pores are created in silica gel during gelation. Then we show that the solid particle arrangement acts on the geometrical pore characteristics (pore volume and pore size distribution). According to the pore size value, the permeability of gels is quite low even if the value of the gel porosity exceeds 95%. Analogous properties can be extended to silica aerogels for which now the solvent is replaced by air. Consequently, and according to their low permeability, light weight aerogels exhibit very striking response to mechanical stresses. Here we report unusual experiments allowing us to estimate the mechanical properties of aerogels thanks to their low value of the average pore size. Moreover, one demonstrates that aerogels may be densified at room temperature using an external isostatic pressure. In that case, the pore size may be tailored with respect to the nature and the characteristics of the starting aerogel. The evolution of the textural properties such as the mean pore size and the specific surface area of these tailored aerogels is investigated as a function of isostatic pressure.

1. Introduction

A gel is the result of the setting up of a solid network in a previously homogeneous liquid. As obtained, the gel which occupies the whole volume of starting liquid is a two-phase material. The solid part concerns the network, and the remaining volume is occupied by the liquid. The pore liquid, according to chemical reactions giving rise to the solid, mainly consists of water and alcohol. Consequently, it is called the solvent. Obviously, the solvent is located within the pores of the gel. The liquid may be replaced by air. Such a change, if uncontrolled, leads to a gel shrinkage which deeply modifies the initial texture. The shrinkage, associated to drying, is minimized if drying is performed under supercritical conditions for the solvent.

The gel formation is the final result of a series of elementary reaction steps. The first step is the formation of particles. Then these particles begin to aggregate and resulting clusters stick together to build up the percolating network. Floating clusters,

---

*The paper presented at the International Conference on Sol-Gel Materials, SGM 2001, Rokosowo, Poland.

**Corresponding author, e-mail: phalippo@crit.univ-montp2.fr.

with time, aggregate to the network. We can say that the texture of the gel network may be considered as achieved when an equilibrium between the solid and liquid chemical species is established.

2. Gel formation

The evolution of the initial liquid toward the gel involves the formation of individual solid particles. These particles appear as a result of a classical nucleation and growth mechanism. However, the nature of the starting solution influences the features of the elementary particles.

Regarding an aqueous solution, the silica solubility is around 100 ppm at room temperature and under neutral conditions. The dissolved silica chemical species are silicic acid molecules, $Si(OH)_4$, which can easily react together, to give rise to more polycondensed species. According to Iler [1], monomers transform into dimers and higher condensed molecules up to cyclic compounds. The cyclic compounds are assumed to give rise to solid particles as a result of an internal condensation of silanol Si–OH groups. The polyion $(Si_8O_{20})^{8-}$ is often assumed as the onset of the particle formation [2]. The size of this colloidal particle is of about 1 nm [1].

As soon as the particle is created, it can aggregate with other surrounding ones or it can grow by surface addition of monomers. Obviously, these two mechanisms occur simultaneously. However, their importance mainly depends on the electric charge borne by the particle surface. The electric charge depends on the pH of the solution. The isoelectric point of silica is obtained when particles are in an aqueous solution of pH at about 2. For pH within the range from 8 to 9, the silica particles are negatively charged and the repulsive forces between particles (measured by the zeta potential) are significant.

Consequently, the particles do not collide and the polycondensation between particles is prevented, so the particles grow without aggregation. In such a case the size of particles can reach 30 nm, a value unusually high. Generally, gels obtained by aggregation in aqueous solution are constituted by particles the size of which varies between 5 and 10 nm.

Regarding gels obtained from organometallic compounds, the situation is not so clear. Organometallic compounds of silicon are transformed owing to two chemical reactions of hydrolysis and polycondensation. The hydrolysis reaction must be carried out by adding a solvent in which organic compound and water are miscible. Alcohol is often used. Consequently, the silica solubility depends on the alcohol/water ratio that is evolving when the gelation proceeds. The monomer, which is soluble in alcohol, reacts with water to give rise to chemical species which, according to the condensation reaction, are constituted by an increasing number of $[SiO_4]$ chemical units. The early solid particles which form in the solution have likely size within the range of 0.5–1 nm. They polycondense very quickly to form the tenuous solid network

of the gel. When the hydrolysis is carried out under weakly acidic or neutral conditions, the size of particles is very small.

Gels prepared from organometallic compounds are the most investigated because they show a high purity and total absence of alkali ions. These cations are known to modify the texture and to induce crystallization if the gel is heat treated. Moreover, with respect to the miscibility of liquids (organometallic compounds/alcohol/water) only a small amount of organosilicon compounds, which transform into solid silica, can be introduced in the starting solution. Gel densities in the range of 0.1 to 0.25 are usually obtained.

In the following sections, we will focus on these kinds of gels or aerogels. The gel establishes according to an aggregation phenomenon of particles. Such aggregation gives rise to a disordered 3D arrangement. The gel texture is generally described by different methods. The first one consists of describing the texture by means of an aggregation of particles having the same size but exhibiting different co-ordination numbers. The second one assumes that these particles are located at the edges of a cubic cell. Another way to build up a structure close to that of gel consists of a cubic cell the edges of which are constituted by cylinders made of dense silica. Recently, description of gel texture has been obtained from computer simulations.

The texture of a gel in its wet state is expected to be preserved by a supercritical drying treatment. The texture of the corresponding aerogel is determined by two experimental characteristics. The first one is the apparent density $r_{a,}$ which is related to the porosity through the relation:

$$r_r = \frac{r_a}{r_s} = 1 - P \tag{1}$$

where r_r is the relative density, r_s the skeletal density (2.2 g/cm^3 for silica gel) and P – the porosity.

Figure 1 shows the apparent density as a function of the volume occupied by one gram of gel.

On the other hand, for particles having the same size, the mean co-ordination number $\bar{n}$ of a particle is related to the porosity by the relation [3]:

$$\bar{n} = 2\exp 2.4(1 - P) \tag{2}$$

which indicates that the mean co-ordination number approaches 2.0 when the porosity approaches 100%. In that case, the texture consists only of linear chains of infinite length.

The texture of gel depends on the aggregation of particles. The mean co-ordination number is within the range from 2 to 3. This value corresponds to a special sequency of particle assembly (Fig. 1).

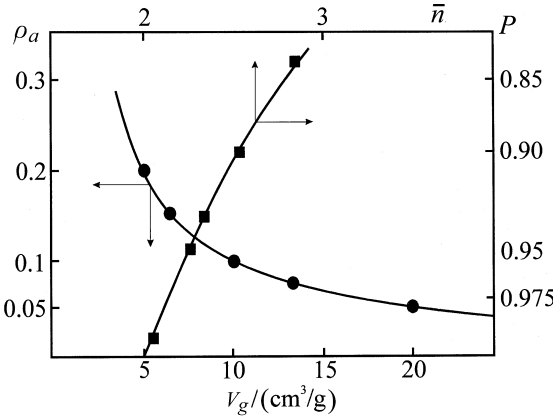

Fig. 1. Bulk density r_a (or porosity P) as a function of the volume occupied by 1 g of a gel; $\bar{n}$ is the mean co-ordination number of elementary particle and V_g the porous volume

Hence, for a porosity of 95%, corresponding to an aerogel having a bulk density of 0.11 g/cm^3, the mean co-ordination number is 2.25. Such a value can be expressed by a sequence of particles for which the number of particles having a co-ordination number of 2 is 3 times higher than that having a co-ordination number of 3. Hence a sequence 3-2-2-3 would describe the texture of the gel (Fig. 2).

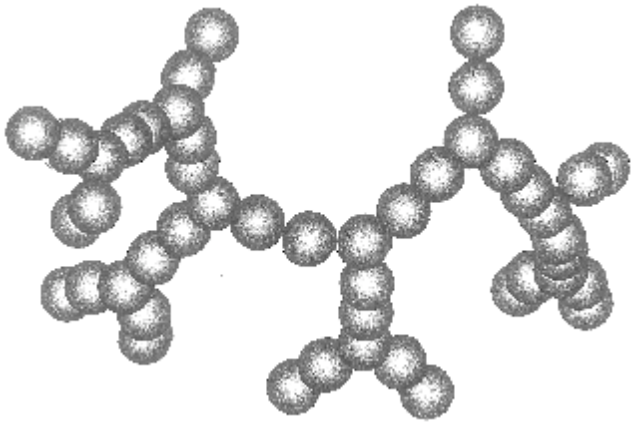

Fig. 2. Schematic texture of a hypothetic gel of a density of 0.11 g/cm^3

The second textural characteristic is the specific surface area S. It is generally obtained from nitrogen adsorption experiments performed at 77 K.

The geometric specific surface area is related to the particle size by the relation:

$$S = \frac{3}{R\, r_s} \tag{3}$$

where R is the radius of particles. Figure 3 shows that the particle size is directly estimated from the specific surface area. However, the experimental surface area is

lower than the geometric one, according to the fact that the adsorbed molecule cannot cover the whole particle surface [4]. An area is lost at the contact between assumed spherical non intersecting particles. A more precise value of the particle radius is obtained using the equation:

$$R = \frac{1375 - \sqrt{(1375)^2 - 4S \times 128.9\,\bar{n}}}{2S} \tag{4}$$

where R is expressed in nm and S in $m^2 \cdot g^{-1}$.

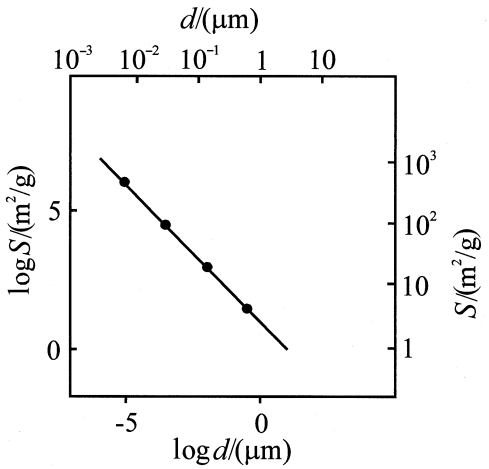

Fig. 3. Specific surface area S as a function of particle size d

Given the specific surface area (400 $m^2 \cdot g^{-1}$) of the previously selected aerogel, the particle size would be of 6.7 nm as estimated from the Eq. (3), while Eq. (4) provides a value of 6.4 nm. Considering that the pore has a dimension of a few particles [5], the pore diameter should be within the range of mesoporosity, easily measured using adsorption–desorption isotherm according to the BJH theory [6].

The model of the cubic cell, the edges of which consist of a chain of pearls, is shown in Fig. 4a. The porosity is related to the number x of spheres located between those forming the vertices of an edge by the relation:

$$r_r = 1 - P = \frac{\pi(1+3x)}{6(1+x)^3} \tag{5}$$

For the selected sample $x = 2$ and the number of particles forming the edge is 3.

Obviously, assuming that there are no necks between particles which are in contact, the specific surface area (400 $m^2 \cdot g^{-1}$) leads to previously calculated particle size (i.e., 6.7 nm). Hence, the edge of the cell has a dimension of 33.5 nm.

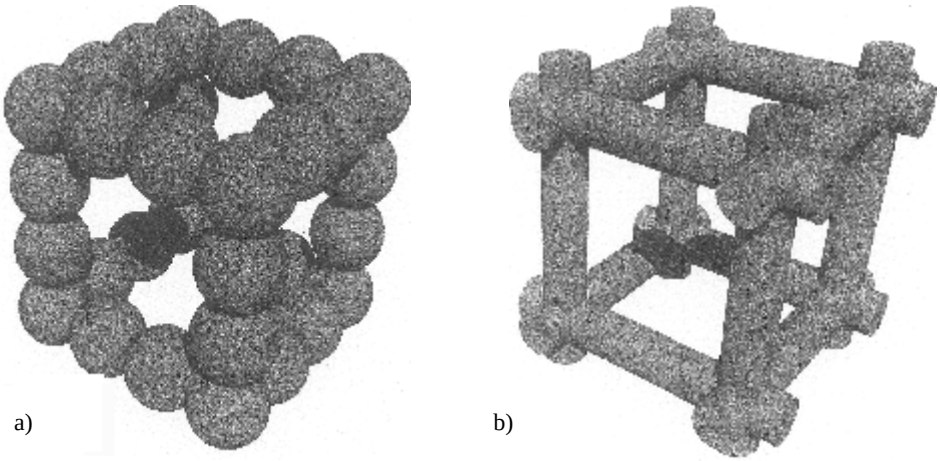

a) b)

Fig. 4. Geometric models proposed for the gel texture:
a) the edges in the form of a chain of pearls, b) cubic cell made of cylinders

Assuming that the pores within the cell (Fig. 4a) can be described by a cylinder, the diameter d_p of the pore corresponds to a circle which can be inscribed in the face of the cell:

$$d_p \approx 27 \text{ nm}$$

Identical calculations can be done using the model of cubic cell made of cylinders [7]. In that case, the porosity is related to the cylinder length l and the cylinder radius a by the relation:

$$r_r = 1 - P = 3\pi\frac{a}{l} - 8\sqrt{2}a^3 \tag{6}$$

In addition, the specific surface area is given by:

$$S = \frac{1}{ar_s}\left[\frac{6\pi l - 24\sqrt{2}a}{3\pi l - 8\sqrt{2}a}\right] \tag{7}$$

The two relations allow us to estimate cell parameters. Given the above reported values of the porosity and of the specific surface area, the cylinder length is equal to 29.5 nm and the cylinder radius equal to 2.1 nm. Consequently, corresponding pore diameter is 25.3 nm, a value close to the previous one.

The last manner to describe the texture of a gel is to simulate such a material using computer models. Computer simulations have been previously used to account for the fractal geometry of gel textures. It has been demonstrated that a fractal dimension of 1.8 is obtained for a diffusion limited cluster–cluster aggregation. Such a fractal di-

mension corresponds well to base-catalysed aerogels. On the other hand, reaction limited cluster–cluster aggregation gives rise to a fractal dimension higher than 2 [8]. The simulated obtained network is expected to describe neutral or acidic catalysed gels.

Small angle X-ray or neutron scattering experiments [9] allow us to measure the fractal dimension. Additionally, the cross over between the fractal and the Porod's regime indicates the size of elementary particles. It has been previously found that the particle size varies between 0.4–0.6 nm for neutral-catalysed aerogels and 1–2 nm for base-catalysed aerogels. The mean pore size may be roughly estimated from the models. It is in the range of 10–50 nm [10].

3. Pore size determination

Up to now, a crude estimate of a mean pore size has been derived with respect to the models. The pore size mainly depends on two parameters: the size of primary particles and the porosity. To summarize, the mean pore size of a gel is within the mesopore domain.

The pore size can be estimated from different techniques. The literature reports a few experiments performed using H NMR in the wet state [11, 12]. This technique permits to separate different kinds of water molecules and the interactions spin–network and spin–spin may be used to identify the amount of water molecules which are located at the surface and those which, located within the pore, diffuse freely. The respective amounts are calculated with the aid of a quite simple model [12], whose application to gels is questionable. The second method used to estimate the pore size distribution is called thermoporometry. It is based on the fact that water within the pores crystallises at the temperature decreasing with the pore size, or more precisely – as a function of the curvature radius of a pore [13]. This technique shows that the mean pore size is related to the sample nature but remains in the mesopore (1–30 nm) range [14].

It is worth noticing that those two mentioned techniques require a gentle solvent exchange to fill the pores with water molecules. Sometimes the solvent exchange induces a network dimensional change. In that case, an experiment with a solvent other than water is needed.

Supercritical drying is a process which allows one to dry the gel theoretically without shrinkage. That occurs in fact for base-catalysed gels which are formed of large particles connected together by large necks. Neutral or acidic gels generally shrink a little during this drying treatment. It is obvious that the texture of aerogels can be analysed by usual adsorption–desorption isotherms of nitrogen (or argon). Both the BET theory [15] for specific surface area and the BJH theory for the pore size distribution are widely used. They confirm that the specific surface area varies between 200 and 800 $m^2 \cdot g^{-1}$ while the pore size distribution spans over a range of 5–30 nm. Recent work demonstrated that these experiments must be carried out with care with respect to the dimensional changes which occur during experiments [16].

It is worth noticing that accurate transmission electron microscopy experiments provide also information about the pore size [17, 18].

The characteristic features of gels are summarized below:

- gels are materials of a low solid content,
- the main phase is fluid (liquid or gas),
- due to a high porosity the elastic moduli are quite small,
- even if the mechanical strength is relatively low, the associated strain is considerable.

A gel exhibits pronounced strains when subjected to very small stresses. In addition, its specific surface area is large and the mean pore size is in the range of mesopores. Consequently, the solid chains of the gel network are very close and are highly reactive with respect to the specific surface.

4. The permeability and its measurement

The permeability D of a porous material having open porosity is a property which accounts for ability of a fluid to go through it.

The fluid flow through a porous material is expressed by Darcy's law:

$$J = -\frac{D}{h} \nabla P \tag{8}$$

Here the flow is considered as laminar. The flux J is inversely proportional to the liquid viscosity h. It depends also on the pressure gradient ∇P applied to liquid. Such a relation applies quite well to liquids flowing through gels. It also accounts for gas diffusion through aerogels. However, for very dense aerogels or partially densified aerogels, the flux corresponds to a peculiar regime called molecular or Knudsen regime. Such a regime establishes when the mean free path of gas molecule becomes higher than the pore diameter [10, 19, 20].

A common way to measure the permeability of a porous material is to estimate the amount of liquid which passes through it per unit of time (Fig. 5).

The experiment works very well for typical porous material. However, because of the small pore sizes, gels show low permeability. In such a case, the flux of liquid is difficult to measure. Usually to improve the measurement of the amount of liquid which flows through the sample the level of liquid is measured using a capillary tube. Moreover, to speed up the experiment a pressure is often applied to the liquid. Unfortunately, for very weakly permeable and compliant material, the pressure causes bending of the sample. The upper part of the material is under a compressive stress. As a result, the size of pores locally reduces and the permeability measurement is erroneous. In addition, the capillary tube may play a role analogous to that of a thermometer and the liquid level can vary according to room temperature, when not precisely controlled.

The gel permeability is easily measured by the thermal expansion method [21]. This method takes advantage of the low mechanical properties of gels. Details of the experimental set-up were previously reported [21]. In few words, the gel containing a non-reactive liquid like alcohol is rapidly heated. During this heating run, the liquid within the pores has no time to escape out of the solid network. It is under compressive stress and, in turn, the solid network is under tensile stress. Because of the low elastic properties of the network, the net result is a solid expansion. If the gel is then maintained at the constant temperature, the liquid has now plenty of time to leave the pores. Consequently, the solid network is under a decreasing stress. The sample contracts down to its initial dimension. Scherer et al. [21] have demonstrated that the experimental curve may be fitted with a theoretical equation containing a hydraulic relaxation time t. This time contains parameters related to the liquid and the solid phases, respectively.

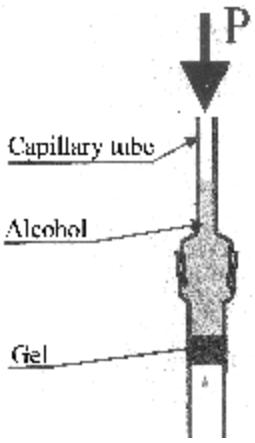

Fig. 5. Usual apparatus allowing the measurement of the permeability of porous material

$$t = \frac{ha^2}{DM} \tag{9}$$

In this expression a is the radius of the rod of a gel and M is the modulus associated with the propagation of longitudinal waves. M is related to the bulk compression K and the shear G moduli according to:

$$M = K + \frac{4}{3}G \tag{10}$$

A simple and elegant method to measure the permeability is the method of three-point bending which does not require special equipment [22]. A sample (cylindrical or prismatic) of gel is suddenly stressed to be deformed down to a selected strain value. In the first instant, the liquid cannot escape from the gel and, consequently, one can say that the sample deforms but its whole volume remains constant. Thus, the sample behaves as an uncompressible fluid. The Poisson coefficient is 0.5 and the apparent Young's modulus E_a:

$$E_a = 2G(1+n) = 3G \tag{11}$$

corresponds to the value of three shear moduli.

Obviously, with time, the liquid can leave the upper compressed surface and enter the lower surface under tension. The Poisson coefficient is 0.2 and the real Young's modulus equal to $2.4G$ is then obtained.

Scherer [22] shows that the curve $W(t)/W(0)$ (where W is the force applied) as a function of time may be fitted with a mathematical expression containing a relaxa-

tion time parameter. This parameter, as indicated before, contains the permeability of a gel. The permeability of gels depends obviously on their nature. For acid-catalysed gels, the permeability is in the range of 10 nm^2. It is twice as high for base-catalysed aerogels. These values confirm a very low permeability of gels. This is the main property responsible for gel cracking occurring during several steps of drying process. For a classical drying, the gel shrinks until the liquid at the network surface enters the pores. During this first step, the liquid flux is driven by the liquid evaporation rate V_E, which can be expressed as the weight loss per unit of time:

$$V_E \propto J = \frac{D}{h}|\nabla P| \tag{12}$$

Consequently, in the case of fast evaporation rates and because of the low gel permeability, the pressure (or stress) gradient between the liquid located at the surface and that in the sample core is high enough to induce cracking [23].

Cracking of large pieces of gels during supercritical drying is also related mainly to permeability, mechanical strength and sample dimensions. The first step of supercritical drying consists of heating the gel in an autoclave. During heating, an expansion is expected. In the case of large pieces of a gel and too fast heating rate, cracking will be observed [24]. Shapes of the cracks are associated with the gel shrinkage. For acid-catalysed gels the shrinkage leads to formation of gels surrounded by syneresis liquids. During heating the liquid flows out freely in all directions. The cracks of the gel do not have a preferred direction. Conversely, a base-catalysed gel does not shrink. Thus, during heating the liquid expands the gel which comes into contact with the walls of an autoclave. Hence, the liquid can only escape through the top surface. Consequently, the gel is under pure tensile stress. It cracks into several slices of about the same thickness (Fig. 6).

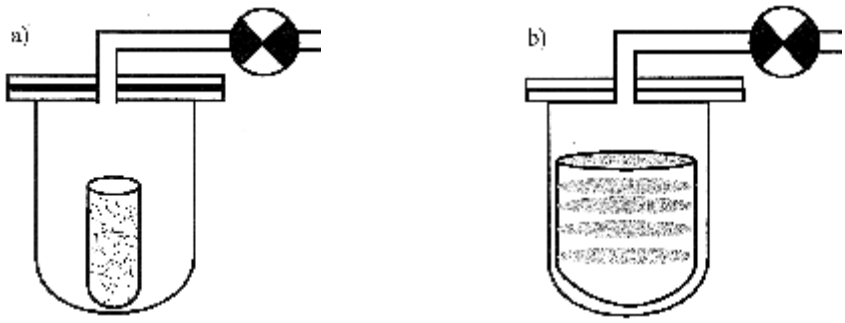

Fig. 6. Cracking of a) neutral- or acid-catalysed gel associated to thermal expansion inside an autoclave, b) base-catalysed gel treated under analogous conditions

In the supercritical drying process when the pressure and temperature are higher than those corresponding to the critical point of the solvent, a supercritical fluid is

obtained. A valve is open to depressurize the autoclave and, consequently, to transform supercritical fluid into gas. If the valve opening is too fast, the superfluid inside the gel remains at a pressure higher than that of superfluid surrounding the sample. The pressure gradient can lead to gel cracking.

5. Advantages of such weakly permeable and porous materials

Because of a low solid content, gels are used to store dangerous liquids which will escape slowly if a leak in the container wall occurs [25]. There also have been attempts to benefit from the thermal insulating properties of aerogels. Investigations concern translucent silica aerogels and highly transparent aerogel plates which are placed between two glass sheets [26].

Some ultraporous aerogels posses elastic modulus so weak that it is quite difficult to measure it. We can take advantages of the low permeability to estimate bulk modulus. An aerogel placed in a non-wetting liquid such as mercury will not have pores invaded by the surrounding liquid. For other porous materials, as the pressure applied to mercury increases, pores having smaller and smaller size will be filled by mercury. For aerogels the mercury cannot enter pores due to their small size. The net effect of the applied pressure is to shrink the sample. In the elastic regime:

$$K = -V\frac{dP}{dV} \tag{13}$$

the bulk modulus K is evaluated from the inverse of the slope of the curve describing the variation of the volume sample as a function of applied pressure [27] (Fig. 7).

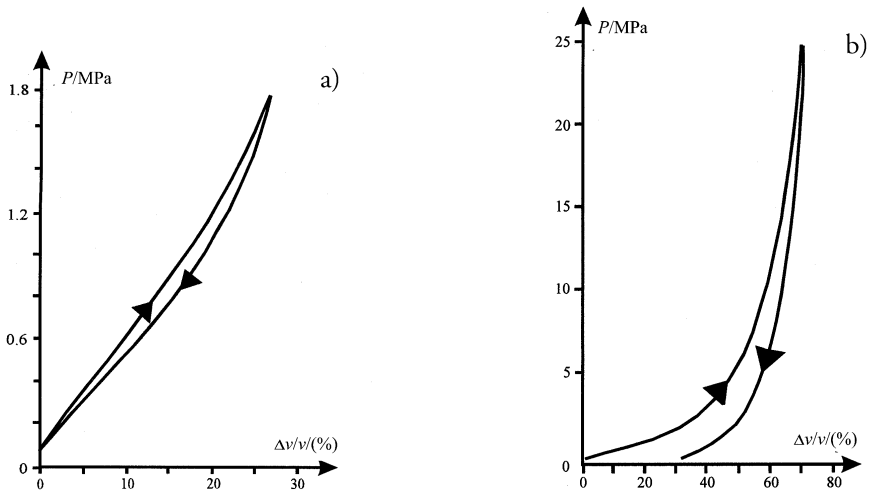

Fig. 7. Relative volume shrinkage as a function of isostatic pressure:
a) elastic regime, b) densification regime

Otherwise, subjecting an aerogel sample to a relative high pressure leads to irreversible volume shrinkage – a real densification occurs [28–30]. Such a room temperature densification depends on the nature of the chemical species covering the pores surface. In order to better understand the densification mechanism a set of base-catalysed fractal aerogels has been prepared. Samples were investigated using small angle X-ray scattering [31]. The curve of the scattering intensity $I(\mathbf{Q})$ as a function of the wave vector $\mathbf{Q}$ on a log scale shows that the slope in the fractal range remains unchanged. The fractal dimension does not vary. The cross-over between the fractal and the Porod's range is not shifted with densification. Thus, the size of primary particles is not modified by room temperature densification resulting from isostatic compression. Note that densification performed by sintering heat treatment leads to the increase in the size of primary particle. The only variation observed concerns the correlation length x which firstly shows a considerable decrease, then tends to a constant value as the sample density increases.

It has been suggested that under compression pressure the fractal blobs interpenetrate. Such a phenomenon requires to break a few chains to permit a better cluster interpretation, but also an increase of the bonds which are created when silanol groups beared by two different chains come into contact. In the first instants the damage caused by bond breaking induces a little decrease of the elastic modulus and correlatively an increase of internal friction [32]. Obviously, for a more pronounced densification, the created bonds become very numerous, the entanglement increases inducing an enhancement of elastic constants.

With respect to this proposed mechanism – mesopores having the largest size and which are likely located between the fractal blobs must disappear first. In order to investigate the pore size distribution as a function of densification, nitrogen adsorption–desorption experiments have been carried out and the pore size obtained from the BJH theory.

During densification a pronounced decrease of the mean size of mesopore is observed (Fig. 8a) while their distribution narrows (Fig. 8b).

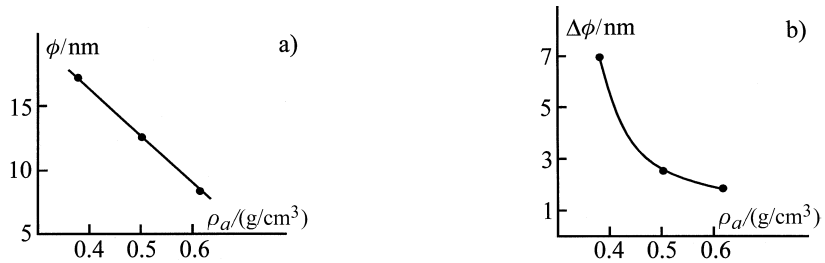

Fig. 8. Density dependence of: a) the mean pore size f, b) the width at middle height Δf of the pore size distribution

Another very striking property of these room-temperature densified aerogels is related to the non-variation of the primary particle size. Obviously, with densification,

the number of particles cannot evolve and consequently the specific surface area remains unchanged [33, 34]. Thus a novel family of materials is obtained. For a given mass of aerogels, the developed surface no more depends on the bulk density. Hence, densified aerogels have a reduced total volume but they exhibit the same specific surface. In other words, the surface per unit volume of material increases as the density rises (Fig. 9).

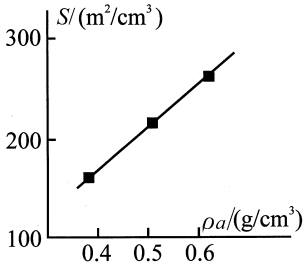

Fig. 9. Evolution of the surface S developed by one cubic centimetre of compressed material as a function of bulk density r_a

6. Conclusion

Gels and aerogels are very porous materials. They have low permeability which decreases as the material shrinks. Any process intended to transform or to modify the gel must be considered according to this specific property. Low permeability has been demonstrated to be useful for determination of elastic properties of very brittle aerogels and to densify them at room temperature. During densification by compression, as the pressure increases, aerogels show the following properties:

- The specific surface area remains constant.
- The elastic constants increase.
- The distribution of pore size narrows.

Aerogels which are room temperature-densified and which additionally exhibit a high specific surface are likely able to sinter easily. Fully dense silica glass is expected to be obtained at a very low sintering temperature and for a low duration of time.

Moreover, the mean pore size may be varied according to the isostatic pressure value. Pore surface may be covered by guest compounds. Such host material can be then thermally sintered to obtain doped silica glass.

References

[1] ILER R.K., *The chemistry of silica*, 1971, New York, Wiley, p. 484.
[2] ENGELHARDT V.G., ALTENBURG W., HOEBBEL D., WIEKER W.Z., Anorg. Allg. Chem., 1977, 418, 43.
[3] MEISSNER H.P., MICHAELS A.S., KAISER R., Ind. Eng. Chem. Process. Des. Div., 1964, 3, 202.
[4] AVERY R.G., RAMSAY J.D.F., J. Coll. Int. Science, 1973, 42 (3), 597.
[5] RAMSAY J.D.F., AVERY R.G., Br. Ceram. Proc., 1986, 38, 275.
[6] BARRET E.P., JOYNER L.G., HALENDA P.P., J. Am. Ceram. Soc., 1938, 60, 309.
[7] SCHERER G.W., J. Am. Ceram. Soc., 1977, 60, 236.
[8] MEAKIN P., JULLIEN R., J. Chem. Phys., 1988, 89 (1), 246.
[9] WOIGNIER T., PHALIPPOU J., VACHER R., J. Mater. Res., 1989, 4, 688.
[10] HASMY A., BEURROIES I., BOURRET D., JULLIEN R., Europhys. Lett., 1995, 29, 567.
[11] BROWNSTEIN K.R., TARR C.E., J. Mag. Resonance, 1977, 26, 17.

[12] GALLEGOS D.P., MUNN K., SMITH D.M., STERMER D.L., J. Colloid. Inter. Science, 1987, 119, 127.
[13] BRUN M., LALLEMAND A., QUINSON J.F., EYRAUD C., Thermochim. Acta, 1977, 21, 59.
[14] DUMAS J., QUINSON J.F., SERUGHETTI J.J., J. Non-Cryst. Solids, 1990, 125, 244.
[15] BRUNAUER S., EMMET PH., TELLER E., J. Am. Ceram. Soc., 1938, 60, 309.
[16] REICHENAUER G., SCHERER G.W., J. Non-Cryst.Solids, 2000, 277, 162.
[17] BOURRET D., Europhys. Lett., 1988, 6–8, 731.
[18] RUBEN G.C., HRUBESH L.W., TILLOTSON T.M., J. Non-Cryst. Solids, 1995, 186, 209.
[19] GROSS J., REICHENAUER G., FRICKE J., J. Phys. D, Appl. Phys., 1988, 22, 1447.
[20] BEURROIES I., BOURRET D., SEMPÉRÉ R., DUFFOURS L., PHALIPPOU J., J. Non-Cryst. Solids, 1995, 186, 328.
[21] SCHERER G., HDACH H., PHALIPPOU J., J. Non-Cryst. Solids, 1991, 130, 157.
[22] SCHERER G.W., J. Non-Cryst. Solids, 1992, 142, 18.
[23] BRINKER C.J., SCHERER G.W., *Sol-Gel Science*, Academic Press, 1990, New York, p. 453.
[24] PHALIPPOU J., SCHERER G.W., WOIGNIER T., BOURRET D., SEMPÉRÉ R., J. Non-Cryst. Solids, 1995, 186, 64.
[25] PAJONK G., TEICHNER S.J., *Principles and applications of pore structural characterization,* Haines and Rossi-Dorier (Eds.), 1985, Bristol, J.W. Arrosmith, p. 227.
[26] FRICKE J., J. Non-Cryst. Solids, 1988, 100, 169.
[27] DUFFOURS L., WOIGNIER T., PHALIPPOU J., J. Non-Cryst. Solids, 1996, 154, 283.
[28] PIRARD R., BLACHER S., BROUERS F., PIRARD J.P., J. Mater. Res., 1995, 10, 2114.
[29] SCHERER G.W., SMITH D.M., QIU X., ANDERSON J., J. Non-Cryst. Solids, 1995, 186, 316.
[30] DUFFOURS L., WOIGNIER T., PHALIPPOU J., J. Non-Cryst. Solids, 1995,186, 321.
[31] BEURROIES I., DUFFOURS L., DELORD P., WOIGNIER T., PHALIPPOU J., J. Non-Cryst. Solids, 1998, 24, 38.
[32] CALAS S., LEVELUT C., WOIGNIER T., PELOUS J., J. Non-Cryst. Solids, 1998, 225, 244.
[33] DIEUDONNÉ PH., PHALIPPOU J., J. Sol-Gel Science and Techn., 1999, 14, 1.
[34] DIEUDONNÉ PH., DELORD P., PHALIPPOU J., J. Non-Cryst. Solids, 1998, 225, 220.